Pergamon

DEEP-SEA RESEARCH
PART I

Deep-Sea Research I 45 (1998) 461–489

The Ekman transfer of nutrients and maintenance of new production over the North Atlantic

Richard G. Williams[a,*], Michael J. Follows[b]

[a] *Oceanography Laboratories, University of Liverpool, Liverpool, L69 3BX, UK*
[b] *Center for Meteorology and Physical Oceanography, 54-1412, MIT, Cambridge, MA 02139, USA*

Received 1 August 1996; received in revised form 10 March 1997; accepted 1 July 1997

Abstract

The maintenance of new production requires a supply of nutrients to the euphotic zone to offset the loss through biological export. The dynamical supply of nutrients is usually discussed in terms of the vertical transfer from nutrient-rich, deep waters. However, the horizontal transfer is important in regions of downwelling over subtropical gyres, where nutrients may be transported across the intergyre boundaries by the surface Ekman drift or geostrophic eddies from the neighbouring nutrient-rich, upwelling regions. The Ekman transfer of nitrate to the euphotic layer is diagnosed from climatology over the North Atlantic. The vertical Ekman supply of nitrate is found to be significant over the subpolar gyre, the tropics and eastern boundary, whereas the horizontal transfer is found to be dominant at the intergyre boundaries. On the northern flank of the subtropical gyre, the Ekman transfer provides a source of nitrate from 0.03 to 0.06 mol N m^{-2} yr^{-1}, corresponding to a contribution to new production of between 0.4 and 0.8 mol C m^{-2} yr^{-1}. This estimate represents a significant fraction of the total new production of typically 1 mol C m^{-2} yr^{-1} suggested by both remote chlorophyll and sediment trap observations. A simplified nitrogen cycle model is used to assess the role of the Ekman supply over the North Atlantic. In the model the Ekman supply of nitrate leads to a plume of nitrate and enhanced productivity extending up to 1000 km into the subtropical gyre from the intergyre boundaries. This lateral scale is controlled by the seasonal cycle of the mixed layer and the remineralisation of the particulate organic fallout.

1. Introduction

New production leads to an uptake of carbon dioxide by the surface ocean and the export of organic matter from the euphotic zone into the deep ocean. This biological

* Corresponding author. Fax: 0044 151 794 4099; e-mail: ric@liv.ac.uk.

0967-0637/98/$19.00
PII: S0967-0637(97)00094-0

consumption and export reduces the concentration of surface nutrients during summer over the North Atlantic (Fig. 1a). While the surface nutrients increase again in winter, partly from entrainment (Fig. 1b), there has to be a net source of nutrients to compensate for the biological export into the underlying main thermocline.

Traditionally, the net supply of nutrients to the euphotic zone is explained in terms of the vertical mixing and upwelling of nutrients from the main thermocline. However, recent tracer release experiments by Ledwell *et al.* (1993) suggest that the vertical mixing in the thermocline is an order of magnitude smaller than previously thought. Vertical advection is certainly important in supplying nutrients to the euphotic zone over upwelling regions, but implies a loss of nutrients over downwelling regions, such as over the subtropical gyre.

Satellite observations of surface chlorophyll suggest that the primary production reaches 30–40 mol C m^{-2} yr^{-1} over the subpolar gyre, off the eastern boundary and parts of the tropics, but reduces to 15 mol C m^{-2} yr^{-1} on the flanks of the subtropical gyre, and reaches a minimum of 5 mol C m^{-2} yr^{-1} in the centre of the subtropical gyre – see Fig. 2 reproduced from Sathyendranath *et al.* (1995). The implied new production over the subtropical gyre, albeit at weaker levels than in the subpolar gyre, cannot be explained by a purely vertical supply of nutrients, and it is necessary to invoke another mechanism.

In our view, nutrients are supplied through *horizontal* advection into the subtropical gyre from the neighbouring, nutrient-rich upwelling regions. This horizontal transfer is likely to occur through an Ekman flux or geostrophic eddy flux *across* the intergyre boundary. In addition, McGillicuddy and Robinson (1997) propose that mesoscale eddies may vertically supply nutrients to the euphotic zone from the nutrient-rich thermocline. There may also be a non-dynamical supply through river runoff, atmospheric deposition (Knap *et al.*, 1986), or nitrogen fixation (Michaels *et al.*, 1996).

In Section 2, we discuss in more detail how the circulation and mixing might supply nutrients to the euphotic zone for an ocean basin, offsetting spring and summer biological export. In Section 3, the vertical and horizontal Ekman supply of nutrients to the euphotic zone is estimated using climatological data over the North Atlantic. In Section 4, a simplified nitrogen cycle model is integrated over the North Atlantic to assess the importance of the Ekman mechanism. In Section 5, the estimates of new production from the climatological Ekman supply are discussed and compared with those from remote sensing and from sediment traps.

2. Dynamical supply of nutrients

Nutrient cycling is discussed here in terms of the total nitrogen, $\mathcal{N}$, defined as the sum of all forms of nitrogen in a sample volume of water (mol N l^{-1}):

$$\mathcal{N} = \underbrace{(NO_3^- + NO_2^- + NH_4 + DON)}_{\text{dissolved}} + \underbrace{(PON)}_{\text{particulate}}, \quad (1)$$

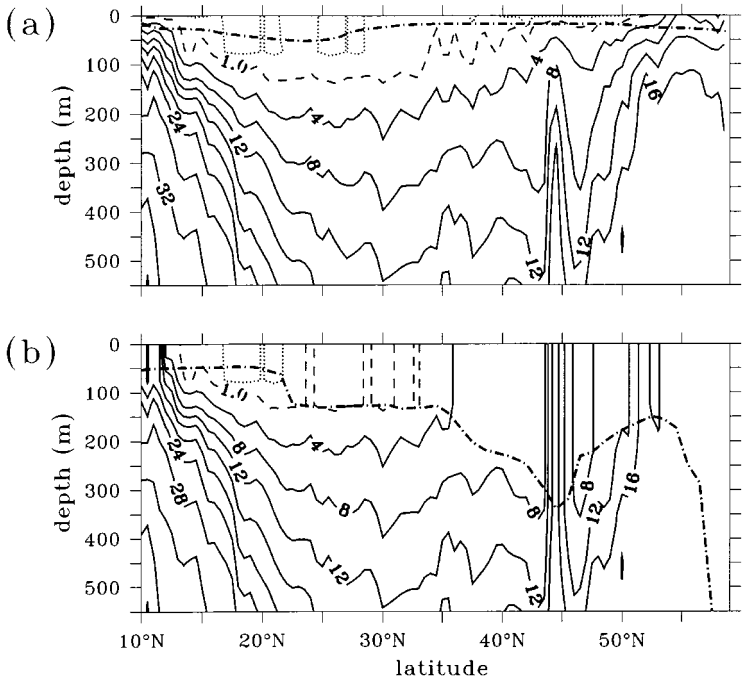

Fig. 1. (a) Observed nitrate (μmol N l^{-1}) section in August 1983 along 35°W in the North Atlantic from the Knorr 104 cruise (taken from Fukumori et al., 1991). The section reveals the depressed nitrate values over the subtropical gyre (typically from 20° to 45°N), and enhanced values in the tropics and subpolar gyre. Contours are in intervals of 4 μmol l^{-1} with extra contours indicating the 1 and 0.1 μmol l^{-1}. (b) Implied nitrate section in March inferred from (a) using the extrapolation method of Glover and Brewer (1988). The thick dashed lines show the thickness of the mixed layer in August and March inferred from the Levitus (1982) climatology.

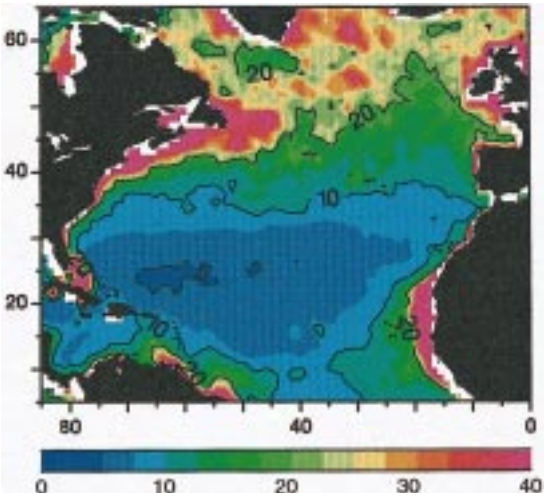

Fig. 2. Annual primary productivity (mol C m^{-2} yr^{-1}) inferred from satellite observations of surface chlorophyll by Sathyendranath et al. (1995) (replotted here). The primary productivity shows maximum values in the subpolar gyre of 30–40 mol C m^{-2} yr^{-1} and reduced values over the flanks and centre of the subtropical gyre of 15–5 mol C m^{-2} yr^{-1}, respectively.

where DON is the dissolved organic nitrogen and PON is the particulate organic nitrogen and includes all forms of biomass. Total nitrogen, $\mathcal{N}$, is conserved during the conversion between organic and inorganic forms, but not during the sinking and remineralisation of particulate matter. The local evolution of $\mathcal{N}$ is given by

$$\frac{\partial \mathcal{N}}{\partial t} + \nabla\cdot(\mathbf{u}\mathcal{N}) + \frac{\partial}{\partial z}\overline{w'\mathcal{N}'} = \nabla\cdot(K\nabla\mathcal{N}) + S. \tag{2}$$

The dynamical supply is controlled by the divergence of the advective fluxes, $\mathbf{u}\mathcal{N}$ (second term on the left-hand side), the vertical divergence of the turbulent fluxes within the mixed layer $\overline{w'\mathcal{N}'}$ (third term on the left-hand side), divergence of eddy fluxes represented by $K\nabla\mathcal{N}$ (first term on the right-hand side); K is the eddy transfer coefficient, $\mathbf{u}$ is the three-dimensional velocity vector, and w is the vertical velocity. The biological influence on nutrients, S, is simply represented as an internal source or sink (second term on the right-hand side), which represents the conversion of organic nutrients to inorganic forms, the subsequent ecological cycling, and eventual fallout from the mixed-layer as particulate organic nitrogen, PON. We define S as the convergence of the vertical flux F of PON:

$$S = -\frac{\partial F}{\partial z}.$$

The above conservation equation for nutrients (2) is non-trivial to solve, and while it has been applied in general circulation models (e.g. see Sarmiento *et al.* (1993) for an ecosystem model of the North Atlantic), it is still useful to discuss the dominant balances with regard to the North Atlantic on seasonal and annual timescales.

2.1. Local, non-advective balance

On a seasonal timescale, the dominant influence on $\mathcal{N}$ within the surface boundary layer is between entrainment and biological processes (see scale analysis in the Appendix) with (2) simplifying to

$$\frac{\partial \mathcal{N}}{\partial t} + \frac{\partial}{\partial z}\overline{w'\mathcal{N}'} = S. \tag{3}$$

Integrating Eq. (3) over the mixed layer of thickness h gives

$$h\frac{\partial \mathcal{N}_m}{\partial t} + \overline{w'}_{z=0} - \overline{w'\mathcal{N}'}_{z=-h} = \int_{-h}^{0} S\,\mathrm{d}z. \tag{4}$$

$\mathcal{N}$ in the mixed layer evolves due to (i) the difference in the turbulent fluxes at the surface and base of the mixed-layer, and (ii) the integrated biological sink within the mixed layer due to the vertical flux of PON through the base of the mixed layer (see Fig. 3).

This relationship represents a disjoint balance, with nutrients decreasing in summer through biological consumption and export ($\int_{-h}^{0} S\,\mathrm{d}z < 0$) and increasing in winter through entrainment.

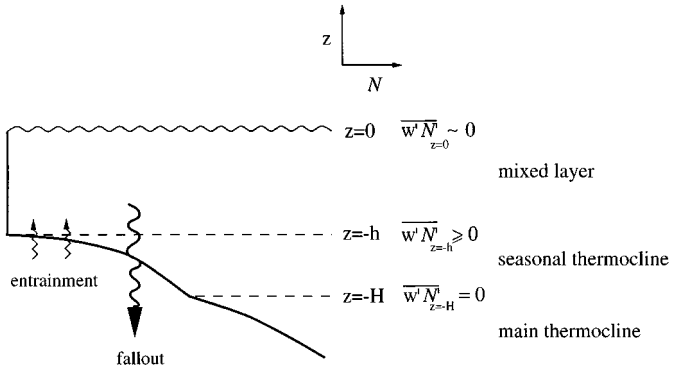

Fig. 3. A schematic nutrient profile for a surface boundary layer. In a local, non-advective balance, the nutrients in the mixed-layer $\mathcal{N}_m$ usually increase through atmospheric deposition $\overline{w'\mathcal{N}'}_{z=0}$ or entrainment $\overline{w'\mathcal{N}'}_{z=-h}$, but decrease through biological fallout. Note that the entrainment flux vanishes at the base of the winter mixed-layer, $z = -H$.

This local balance might be adequate to describe changes on seasonal timescales, but *cannot* suffice over several annual cycles. *If* the nutrient balance (4) is integrated over the seasonal boundary layer (defined by the maximum thickness, H, of the winter mixed layer), then the entrainment flux vanishes, $\overline{w'\mathcal{N}'}_{z=-H} \equiv 0$, as by definition there is no further deepening beyond this level (Fig. 3). Thus, entrainment does *not* provide a source of nutrients for the whole of the seasonal boundary layer, but instead simply re-distributes nutrients within the seasonal boundary layer. In addition, if surface inputs of nutrients, such as atmospheric deposition and river runoff, are also assumed negligible, $\overline{w'\mathcal{N}'}_{z=0} \sim 0$, then Eq. (4) reduces to

$$\frac{\partial}{\partial t}\int_{-H}^{0} \mathcal{N}\,\mathrm{d}z \sim \int_{-H}^{0} S\,\mathrm{d}z. \tag{5}$$

This balances implies that the nutrients within the surface boundary layer will be eventually exhausted by any biological export into the main thermocline ($\int_{-H}^{0} S\mathrm{d}z < 0$). Clearly, the local, non-advective balance is inadequate over several annual cycles. We now focus on the advective processes that might supply nutrients to the seasonal boundary layer and offset the biological consumption and export.

2.2. Vertical transfer

Nutrients are generally thought to be supplied to surface waters from the nutrient-rich deeper water by vertical diffusion or advection. For example, Munk (1966) used a one-dimensional model to explain the vertical distribution of properties in the Pacific and diagnosed that the required vertical diffusivity is $\sim 10^{-4}\,\mathrm{m^2\,s^{-1}}$. Such high vertical diffusivities have frequently been employed in order to sustain production levels in one-dimensional ecosystem models.

However, deliberate tracer release experiments have shown that the diapycnal diffusivity in the subtropical gyre thermocline is an order of magnitude smaller, $\sim 10^{-5}\,m^2\,s^{-1}$ (Ledwell *et al.*, 1993). This reduced value suggests that advection is likely to be more important than vertical diffusion (see scaling in Appendix A).

The large-scale vertical motion is controlled by the wind-stress field, which drives upwelling in the subpolar gyre and along some eastern boundaries, and downwelling in the subtropical gyre (Fig. 4). This pattern of vertical motion broadly agrees with surface waters being nutrient-rich in the subpolar gyre and along eastern boundaries. McClain and Firestone (1993) argue that there is a correlation between maps of remotely-sensed ocean colour (interpreted as biomass) and Ekman suction.

While surface nutrient concentrations are less in the subtropical gyre than in the subpolar gyre, they are *not* completely depleted in winter, even though there is biological activity in the spring and early summer (see Figs. 1 and 2). This poses the question: how are the nutrients supplied to surface waters in regions of widespread downwelling, such as in the subtropical gyre? In our view, it is necessary to consider both horizontal and vertical processes to answer this question, although McGuillicuddy and Robinson (1997) alternatively suggest that vertical upwelling from the smaller eddy/frontal scale is important.

2.3. Horizontal transfer

Nutrients are transferred by the horizontal circulation, as well as by the vertical circulation. With regards to the supply of nutrients to the euphotic zone of the subtropical gyre, there may be a *horizontal* transfer from the neighbouring, nutrient-rich subpolar gyre or tropics through surface Ekman currents, time-mean geostrophic flow, and time-dependent geostrophic eddies.

The mechanism most likely to consistently supply nutrients to the euphotic zone of the subtropical gyre is the surface Ekman flux (Fig. 5a). Westerly winds induce a southwards volume flux along the subtropical/subpolar boundary, which reaches $\sim 5\,Sv$ ($1\,Sv = 10^6\,m^3\,s^{-1}$) when integrated across the basin. This southwards Ekman flux transfers fresher water into the subtropical gyre and probably accounts for the freshening seen in the mixed layer during summer over the North Atlantic

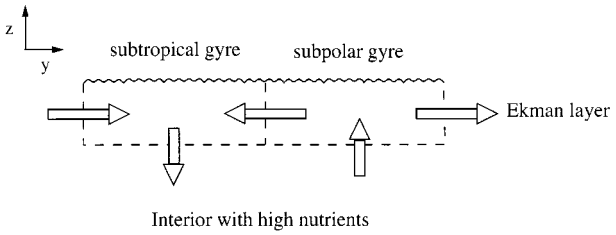

Fig. 4. A schematic meridional section showing the Ekman transfers through a subtropical and subpolar gyre. The wind forcing leads to a horizontal divergence over the subpolar gyre, inducing upwelling, and a divergence over the subtropical gyre, inducing downwelling.

(as reported by Neumann, 1940; Taylor and Stevens, 1980; Leach, 1990); the Ekman advection is probably masked by the convective mixing occurring during winter. Such Ekman fluxes should likewise transfer nutrients into the subtropical gyre from upwelling regions in both the subpolar gyre and the tropics.

The time-mean geostrophic flow in the interior is unlikely to play a comparable role in transferring nutrients across the inter-gyre boundary, since the depth-integrated meridional geostrophic flow should vanish along the zero Ekman pumping line if Sverdrup balance holds. However, there may still be a time-mean geostrophic flux of nutrients in the western boundary currents. Once nutrients are transferred into the gyre, the interior geostrophic flow will become important in advecting them around the rest of the gyre.

The time-dependent geostrophic flow consisting of eddies and meandering currents might be important in transferring properties between the gyres. Baroclinic instability of a front leads to the formation and exchange of warm and cold eddies across the front. If cold-core eddies contain higher nutrients, then their equatorwards movement leads to an equatorwards flux of high nutrients (Fig. 5b). This eddy-driven transfer might be particularly important across intense currents, such as the Gulf Stream and Antarctic Circumpolar Current, as well as along the inter-gyre boundaries.

In the following Section 3, we use climatological data to estimate the Ekman-driven transfer of nitrate, and in Section 4, use a simplified nitrogen model to assess the importance of this mechanism.

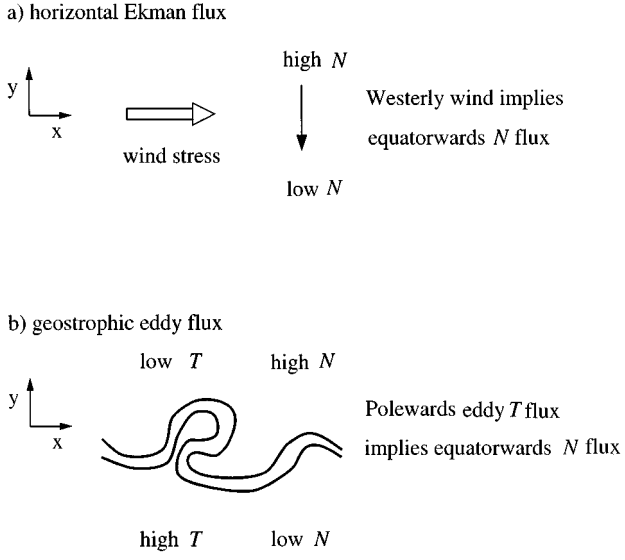

Fig. 5. A schematic figure showing mechanisms that transfer nutrients horizontally across an inter-gyre boundary: (a) an eastward wind-stress drives an equatorward surface Ekman flux, which leads to high nutrients in the subpolar gyre being swept into the subtropical gyre, (b) the instability of a front leading to an exchange of warm and cold eddies implies an equatorward flux of nutrients assuming that there are higher nutrients in cold water.

3. Estimating the Ekman supply of nitrate from climatology

3.1. The supply of nitrate to the Ekman layer

In these diagnostics, we focus on the supply of nitrate to the euphotic zone by the vertical and horizontal Ekman flux, rather than total nitrogen $\mathcal{N}$ since nitrate NO_3^- is available from climatology. Rewriting Eq. (2) in terms of NO_3^- and integrating over the Ekman layer of thickness h_e gives

$$\frac{\partial}{\partial t}\int_{-h_e}^{0} NO_3^- \, dz = -\int_{-h_e}^{0} \nabla\cdot(\mathbf{u}NO_3^-)\,dz - [\overline{w'NO_3^{-\prime}}]_{z=-h_e}^{z=0} + \int_{-h_e}^{0} \nabla\cdot(K\nabla NO_3^-)\,dz + \int_{-h_e}^{0} S_{NO_3^-} dz. \tag{6}$$

The term denoting biological processes, $S_{NO_3^-}$, now refers specifically to processes affecting the nitrate concentration. As the integration is over the Ekman layer, the entrainment term is now non-zero over the time-mean (whereas the term vanishes over the entire seasonal boundary layer).

The velocity field $\mathbf{u}$ may be separated into a geostrophic flow $\mathbf{u}_g$ extending over the whole water column and an Ekman horizontal velocity, $\mathbf{u}_e$, confined within the shallow Ekman layer. The Ekman supply of nitrate in the Ekman layer in Eq. (6) is given by[1]

$$-\int_{-h_e}^{0} \nabla\cdot(\mathbf{u}_e NO_3^-)\,dz = -\nabla\cdot(\mathbf{U}_e NO_{3m}^-) + w_e NO_{3m}^-, \tag{7}$$

where subscript m denotes a value in the mixed layer and $\mathbf{U}_e$ is the horizontal Ekman volume flux per unit length. The horizontal and vertical supply are represented by the first and second terms on the right-hand side of Eq. (7). As the divergence of the horizontal volume flux, $\mathbf{U}_e$, drives the vertical Ekman velocity, $\nabla\cdot\mathbf{U}_e = w_e$, the total Ekman supply of nitrate from Eq. (7) can be written more concisely as

$$-\int_{-h_e}^{0} \nabla\cdot(\mathbf{u}_e NO_3^-)\,dz = -\mathbf{U}_e\cdot\nabla NO_{3m}^-. \tag{8}$$

Consequently, the annual Ekman supply of nitrate is given by

$$-\int_{0}^{\text{year}} \mathbf{U}_e\cdot\nabla NO_{3m}^- \, dt. \tag{9}$$

[1] The Ekman supply of nitrate is formally evaluated over the Ekman layer, but the only assumption made here is that the Ekman layer is not thicker than the instantaneous mixed layer. Therefore, the subsequent diagnostics of the Ekman nitrate supply to the Ekman layer are equivalent to that for the mixed layer and euphotic zone.

In a steady state, this supply of nitrate by the Ekman flow together with the other potential sources in Eq. (6) to this layer (such as geostrophic advection, entrainment, atmospheric deposition, and diffusion) must balance the annual consumption and ultimate export of nitrate by biological processes from the Ekman layer:

$$\int_0^{\text{year}} \int_{-h_e}^{0} S_{\text{NO}_3^-} \, \mathrm{d}z \, \mathrm{d}t. \tag{10}$$

3.2. Climatological diagnostics

Climatological estimates are now made of the Ekman supply of nitrate, which may be helping to maintain new production over parts of the North Atlantic.

The algorithm used to evaluate the Ekman supply of nitrate on a 1° grid from Eq. (9) is as follows:

(1) the mixed-layer depth $h(x, y, t)$ is diagnosed every month over the North Atlantic from the Levitus (1982) climatology (defined by the depth where σ_θ increases by 0.125 from the surface value). For example, the mixed-layer thickness for April is shown in Fig. 6a, with values typically of 50 m in the southern half of the subtropical gyre increasing to 500 m in the subpolar gyre.

(2) The annual-mean profiles, $\text{NO}_{3\,\text{annual}}^-$, are taken from the climatology of Conkright *et al.* (1994). This dataset is biased towards summer, when most observations were taken. Following Glover and Brewer (1988), the nitrate within the mixed layer, $\text{NO}_{3\text{m}}^-$, may be estimated from h and $\text{NO}_{3\,\text{annual}}^-$ using an extrapolation method

$$\text{NO}_{3\text{m}}^-(x, y, t) = \text{NO}_{3\text{annual}}^-(x, y, h(x, y, t)). \tag{11}$$

For example, the implied mixed-layer nitrate in April using the extrapolation method is shown in Fig. 6b, revealing high values, typically of 10 $\mu\text{mol N l}^{-1}$, in the subpolar gyre and only 1 $\mu\text{mol N l}^{-1}$ in the subtropical gyre.

(3) The Ekman volume fluxes are evaluated from the monthly wind-stress field from Isemer and Hasse (1987). The horizontal Ekman volume flux is given from $\mathbf{U}_e = (\mathbf{k} \times \tau)/(\bar{\rho} f)$, and their divergence induces the vertical Ekman velocity at the base of the Ekman layer, $w_e = \nabla \cdot \mathbf{U}_e = (\mathbf{k}/\bar{\rho}) \cdot \nabla \times (\tau/f)$; here f is the Coriolis parameter, $\mathbf{k}$ is the vertical unit vector, τ is the wind-stress, and $\bar{\rho}$ is a reference density. The Ekman upwelling velocity in April is shown in Fig. 6c with the zero-line separating the subpolar and subtropical gyres, and the upwelling and downwelling respectively being typically 50 m yr^{-1}.

Fig. 6. Mixed-layer distributions in April: (a) thickness of mixed layer (m) diagnosed from the Levitus (1982) climatology, (b) nitrate concentration in the mixed layer ($\mu\text{mol N l}^{-1}$) diagnosed using the extrapolation method of Glover and Brewer (1988) from climatological nitrate of Conkright *et al.* (1994), (c) the Ekman upwelling velocity (m yr^{-1}) diagnosed from the wind-stress climatology of Isemer and Hasse (1987).

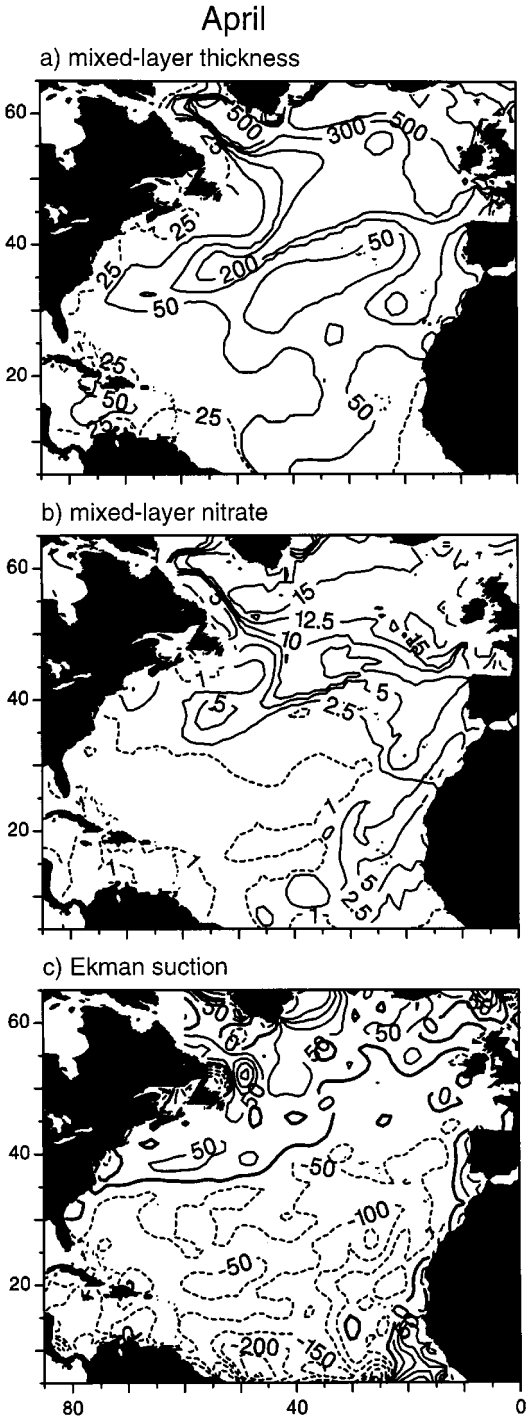
April
a) mixed-layer thickness
b) mixed-layer nitrate
c) Ekman suction
60
40
20
80
40
0

(4) The supply of nitrate from the Ekman transfer, $-\mathbf{U}_e \cdot \nabla NO_{3m}^-$, is evaluated using up-wind differencing at every 1° grid-point.

3.2.1. The Ekman supply of nitrate in April

We firstly discuss the Ekman supply of nitrate during April, as this term is largest then when there are strong winds and high nitrate concentrations in the deep mixed-layers.

The vertical Ekman supply of nitrate, $w_e NO_{3m}^-$, during April is shown in Fig. 7a. There are positive values in the upwelling regions of the subpolar gyre and off Africa in the tropics, with negative values in the downwelling regions in the subtropical gyre. The marked zero line reflects that of w_e in Fig. 6c. The vertical flux of nitrate into the euphotic zone reaches 20×10^{-9} mol N m^{-2} s^{-1} (red in Fig. 7a) in the upwelling regions, whereas it reaches -5×10^{-9} mol N m^{-2} s^{-1} in the subtropical gyre (dark blue in Fig. 7a). This loss of nitrate in the subtropical gyre is significant and is unlikely to be entirely compensated for by processes such as vertical diffusion or atmospheric deposition.

The horizontal supply of nitrate, $-\nabla \cdot (\mathbf{U}_e NO_{3m}^-)$, in April is shown in Fig. 7b. The horizontal transfer induces a loss of nitrate over parts of the subpolar gyre and tropics, but *supplies* nitrate in the subtropical gyre (blue and red in Fig. 7b, respectively). There are strikingly large values along the boundary of the subtropical and subpolar gyres (the red bands in Fig. 7b), reaching 20×10^{-9} mol N m^{-2} s^{-1}, which reflect the transfer of nitrate-rich water from the subpolar into the subtropical gyre. This Ekman-induced transfer is directly analogous to the observed equatorward transfer of low salinity waters. There is also a large Ekman supply at the tropical/subtropical boundary, where the westward wind drives a poleward flux of tropical waters with high nutrients.

The resulting total supply of nitrate by the Ekman transfer, $-\mathbf{U}_e \cdot \nabla NO_{3m}^-$, in April is shown in Fig. 7c. The total Ekman supply is larger in the subpolar gyre, but there are now also widespread regions of supply in the subtropical gyre. Negative values indicate regions where the Ekman transfer leads to a net loss of nitrate in the surface waters – other processes must be important here (entrainment, geostrophic advection, eddy transports or atmospheric deposition) if there is to be any new production.

3.2.2. The annual Ekman supply

The annual supply of nitrate by Ekman transfer is evaluated by summing the monthly contributions from October to April and dividing by 12, providing a lower bound estimate. The summer period is not included in the summation as biological processes will deplete the surface nitrate and may even remove it entirely – the extent of this summer period is defined after examining the series of chlorophyll and nitrate sections from 40°N to 54°N in the mid-Atlantic shown by Strass and Woods (1991).

The resulting map of annual Ekman supply is shown in Fig. 8a and reveals positive values over most of the basin. In the subpolar gyre, there are higher values of 20×10^{-9} mol N m^{-2} s^{-1} to the west, compared with 5×10^{-9} mol N m^{-2} s^{-1} to the east (marked red and green in Fig. 8c, respectively). In the subtropical gyre, the Ekman supply shows a narrow band of high values (marked red) with typical values elsewhere

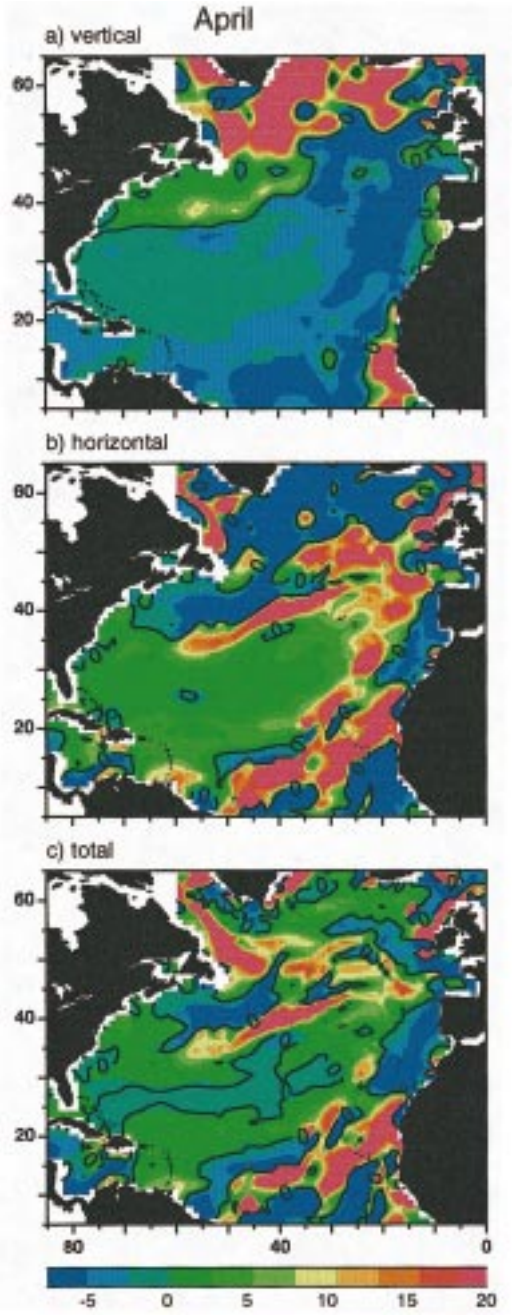

Fig. 7. The Ekman supply of nitrate during April (10^{-9} mol N m^{-2} s^{-1}): (a) the vertical Ekman nitrate flux $w_e NO_{3m}^-$, (b) the convergence of the horizontal Ekman nitrate flux $-\nabla\cdot(\mathbf{U}_e NO_{3m}^-)$, and (c) the convergence of the total Ekman nitrate flux $-\mathbf{U}_e\cdot\nabla NO_{3m}^-$. Note that positive values represent a supply of nitrate to the Ekman layer.

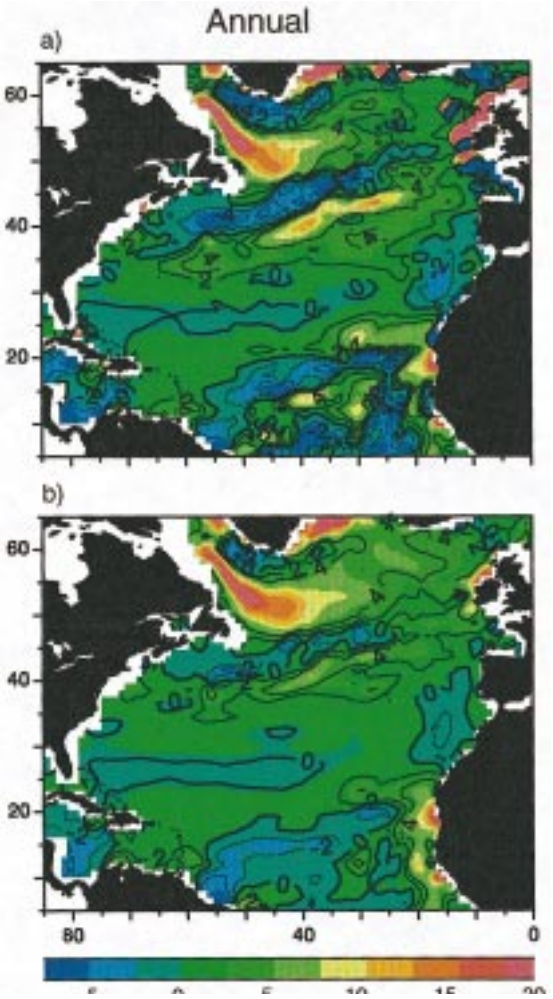

Fig. 8. The annual Ekman supply of nitrate (10^{-9} mol N m^{-2} s^{-1}) estimated by summing the monthly contributions from October to April and dividing by 12, where nitrate in the mixed layer is estimated using (a) the extrapolation or (b) the integral method of Glover and Brewer (1988).

reaching from 2 to 4×10^{-9} mol N m^{-2} s^{-1} on the northern flank of the gyre (these annual values are equivalent to 0.06 and 0.12 mol N m^{-2} yr^{-1}).

The annual mean values are less than those estimated in April, since the intergyre transfer is a maximum at the end of winter when the westerly winds are strong and the surface nitrate gradients are enhanced. Again, in the annual mean, there are some negative values, particularly along the Gulf Stream, the centre of the subtropical gyre and parts of the tropics. These reflect the contribution of other supply processes (entrainment, geostrophic advection, eddy transfer or atmospheric deposition) or, alternatively, error in our diagnosis of the climatological data. The spatially averaged Ekman contribution to new production over the entire domain is positive and reaches 1.2×10^{-9} mol N m^{-2} s^{-1} (the area of domain being 2.3×10^{13} m^2).

The annual Ekman supply is also evaluated using the integral method for estimating NO_3^- in the mixed layer by Glover and Brewer (1988), where

$$NO_{3m}^-(x, y, t) = \frac{1}{h(x, y, t)} \int_{-h}^{0} NO_{3annual}^-(x, y)\, dz. \tag{12}$$

The integral method predicts lower NO_3^- values in the winter mixed layer than the extrapolation method (but does conserve NO_3^- for a deepening of the mixed layer). The resulting estimate of the annual Ekman supply using the integral method has smaller maxima (Fig. 8b) than the extrapolation method, although the spatially averaged flux is slightly higher, reaching 1.5×10^{-9} mol N m^{-2} s^{-1} over the entire domain.

3.3. *Lateral extent of the Ekman supply within the subtropical gyre*

The question arises as to how far the Ekman transfer can significantly influence new production into the interior of a subtropical gyre? After nutrients are transported in the Ekman layer across the boundaries of the subtropical gyre, they will subsequently be advected by *both* the geostrophic and Ekman flow. However, nutrients will be rapidly consumed and exported through biological fallout during summer. Thus, one might expect this Ekman supply to be significant over a meridional scale of $L \sim V\mathscr{T}$ emanating from the intergyre boundary, which is only 150 km for a meridional velocity of $V \sim 1$ cm s^{-1} and $\mathscr{T} \sim 6$ months, assuming the latter as the timescale over which nutrients persist in the surface layers. However, most of the biological fallout is remineralised within the underlying seasonal thermocline. In this case, the remineralised nutrients can be advected further into the gyre interior and re-entrained into the mixed layer during the following winter. Thus, the nutrient signal might extend up to $L \sim 1000$ km from the intergyre boundaries if the re-entrainment of nutrients leads to the timescale increasing to 3 yr. In the following section, we examine this hypothesis using a nitrogen cycle model integrated over the North Atlantic.

4. A nutrient cycle model for the North Atlantic

The supply of nutrients to the subtropical gyre is now investigated using a simplified nitrogen cycle model with a resolved seasonal cycle and parameterised biology.

Idealised experiments are conducted to highlight the importance of the Ekman transfer and remineralisation of nutrients.

4.1. The transport model

The nitrogen cycle model is driven by off-line velocity fields from the $1.0^\circ \times 1.2^\circ$ CME (Community Modelling Effort) general circulation model (Holland and Bryan, 1994). Model fields from the CME are stored every three days providing a fully resolved seasonal cycle. In these experiments, the domain is restricted to the upper 1600 m and ranging from the equator to 65°N. The nitrogen cycle model integrates the advection–diffusion equation for total nitrogen, $\mathcal{N}$, using these velocities with upstream finite differencing:

$$\frac{\partial \mathcal{N}}{\partial t} + \nabla\cdot(\mathbf{u}\mathcal{N}) - \nabla\cdot(K_h \nabla_h \mathcal{N}) - \frac{\partial}{\partial z}\left(K_v \frac{\partial \mathcal{N}}{\partial z}\right) = S. \tag{13}$$

In addition, the thickness of the mixed layer is diagnosed from the density profile in the general circulation model with $\mathcal{N}$ vertically homogenised within this layer and any deepening of the mixed layer leading to entrainment fluxes; see Eq. (A.2) in Appendix A. The off-line tracer model is described in more detail in previous studies by Williams *et al.* (1995) and Follows *et al.* (1996); eddy transfers are crudely represented by lateral and vertical diffusivities of $K_h = 1000\,\mathrm{m^2\,s^{-1}}$ and $K_v = 10^{-5}\,\mathrm{m^2\,s^{-1}}$.

Inflow through the open boundaries of the model brings $\mathcal{N}$ into the domain. The boundary conditions are assumed to be uniform in longitude and are taken from averaged observed NO_3^- profiles:[2] the equatorial profile is from the average of stations 42, 46, 109, and 111 from GEOSECS, and the northern profile is from the average of stations 160, 161, 163, 164, 193, 195, 197, 198 from TTO (Bainbridge, 1981; Brewer, *et al.*, 1986). The lower boundary condition of NO_3^- at 1600 m is set by a linear interpolation of the meridional boundary conditions at that depth.

4.2. Nitrogen cycling parameterisations

Simple parameterisations of biogeochemical processes are implemented into the tracer model.

4.2.1. Export and new production

The biological export of nitrogen from the mixed layer is assumed to be nutrient and light limited, and is simply parameterised as a loss of $\mathcal{N}$ from the mixed layer,

$$S = -\lambda \frac{h_e}{h} \mathcal{N}_m, \quad z \geqslant -h,$$

[2] These boundary conditions ignore the possible contribution of DON, which is neglected due to lack of observations. This discrepancy might lead to the import of nitrogen in the surface waters being underestimated, although the errors at depth are likely to be small.

which depends on the available nutrients, $\mathcal{N}_m$, an inverse timescale, λ, and the ratio of the thickness of the euphotic zone h_e (set to 100 m in the model) and the mixed layer. The inverse timescale λ is assumed to vary with insolation (and hence in space and by season) according to

$$\lambda = A\,I(y,t),$$

where I is the vertical integral of photosynthetically active radiation over the euphotic zone (with the extinction coefficient of solar radiation in seawater assumed to be $0.05\ m^{-1}$). The flux of solar radiation just below the surface of the ocean is determined as a function of latitude and season from astronomical data (Paltridge and Platt, 1976) and an assumed planetary albedo. The constant factor, A, is tuned so that the fallout timescale is about $1/\lambda = 1$ month during summer, but increases (through the reduction in solar radiation) to many years at higher latitudes during winter.

Here, we define export production as the flux of nitrogen removed from the euphotic zone as particulate fallout, which is given here by

$$F(-h_e) = -\lambda h_e \mathcal{N}_m.$$

The area-average export production and new production are equivalent in the time mean (Dugdale and Goering, 1967).

4.2.2. Remineralisation

Remineralisation is assumed to occur below the mixed layer with the downwards vertical flux of PON chosen to decrease exponentially with depth (similar to the scheme of Najjar and Sarmiento, 1992),

$$F(z) = F(-h_e)\,e^{(h+z)/z^*},$$

and the resulting biological source of $\mathcal{N}$ in the thermocline given by the convergence of the particle flux,

$$S = -\frac{\partial F(z)}{\partial z}, \quad z \leqslant -h.$$

The scale height for remineralisation, z^*, is assumed to be 400 m following sediment trap observations of Lohrenz et al. (1992) from the Sargasso Sea, which indicate a scale height of a few hundred metres, and the data of Martin *et al.* (1987) in the northeast Pacific, which suggest $z^* \sim 400$ m (although the authors chose a slightly different function to fit their data).

4.3. Model experiments

The model is initialised with a uniform value of $\mathcal{N} = 20\ \mu mol\ N\,l^{-1}$ and integrated for 600 yr, by which time a steady repeating annual cycle in the $\mathcal{N}$ field has developed. The model does not include any atmospheric deposition or frontal-scale upwelling and has a relatively small vertical diffusion. The model results are now described

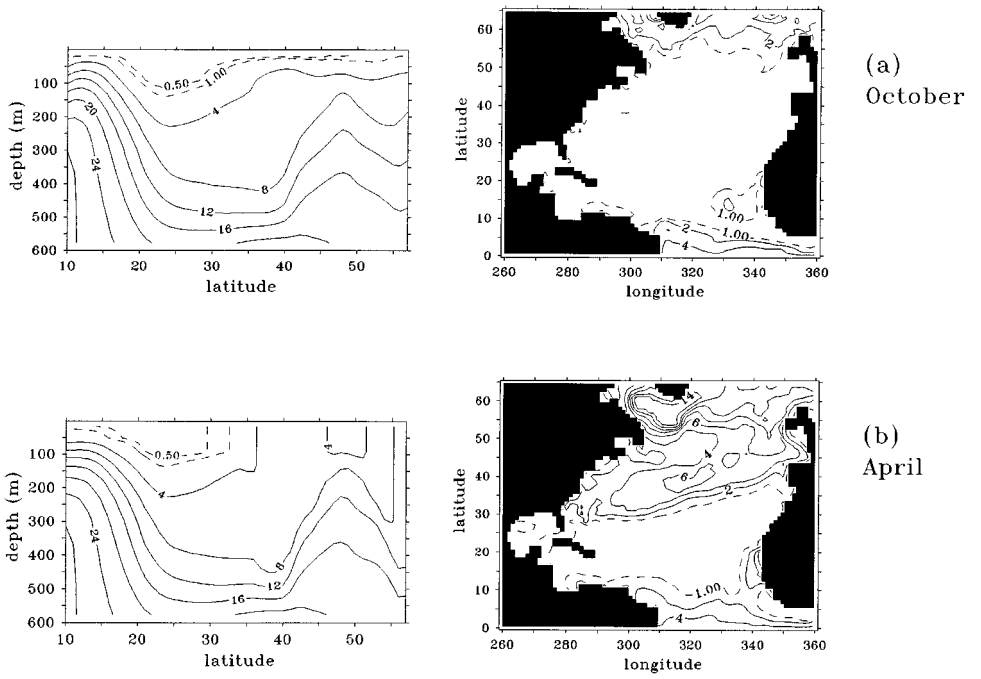

Fig. 9. Modelled total nitrogen, $\mathcal{N}$ (μmol N l^{-1}) in (a) October and (b) April for a meridional section at 22°W and maps within the mixed layer. $\mathcal{N}$ is depressed over the subtropical gyre and enhanced over the tropics and subpolar gyre. The surface nutrients have enhanced concentrations in April and lower values in October with nearly complete depletion over the subtropical gyre.

firstly for a reference integration (using the previously given parameters), and secondly for sensitivity experiments examining the importance of the remineralisation scale for the horizontal transfer and export production.

4.3.1. Seasonal cycle

The model sections of $\mathcal{N}$ in October and April at 22°W shown in Fig. 9 appear broadly similar to the observed fields and diagnostics of NO_3^- in Fig. 1.[3] There are low surface nitrogen concentrations in the subtropical gyres, which are pumped down into the thermocline, and higher surface nitrogen in the subpolar gyre and equatorial regions. The seasonal cycle leads to a reduction in the surface nutrients during summer, but they increase again in winter. This seasonal cycle is evident in the mixed-layer maps of $\mathcal{N}$ showing the region of low nutrient surface waters expanding in autumn and contracting in spring (Fig. 9).

[3] This comparison of NO_3^- and $\mathcal{N}$ should be considered with caution, since $\mathcal{N}$ represents total nitrogen, including some component of dissolved and particulate organic nitrogen not included in the observed NO_3^- fields. The comparison is likely to be more appropriate at depth, where the organic fraction is probably smaller.

4.3.2. Advection of nitrogen

Fig. 10 depicts the annual mean model tendencies, integrated from the surface to 35 m, due to the processes of advection, entrainment and particulate export. Over the subpolar gyre and northern flank of the subtropical gyre, there is a three way balance with supply of nutrients by advection and entrainment balancing the loss by

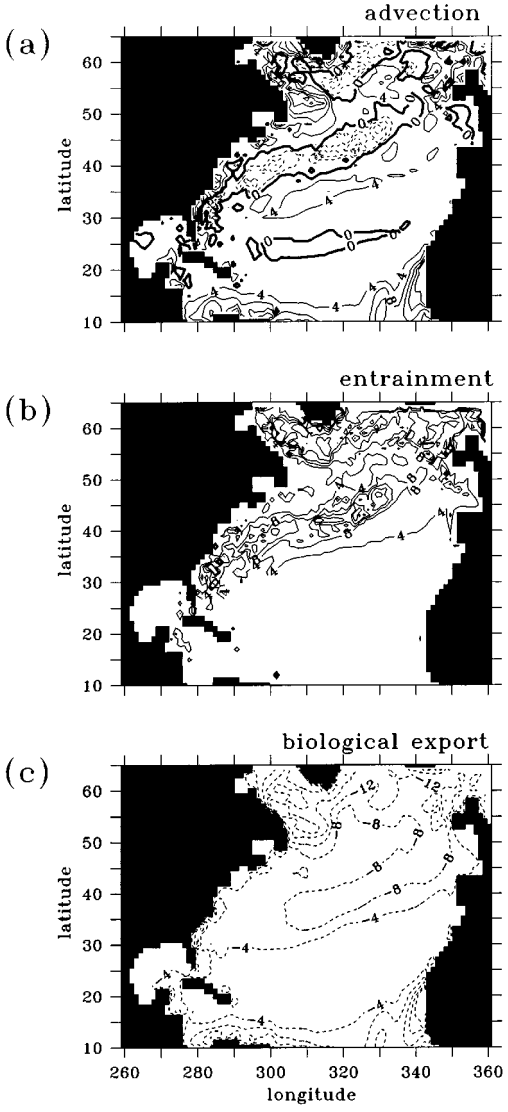

Fig. 10. Modelled annual supply of $\mathcal{N}$ (10^{-9} mol N m^{-2} s^{-1}) in the Ekman layer (over the uppermost 35 m): (a) advection including Ekman and geostrophic, (b) entrainment and (c) biological export.

biological export. However, over the rest of the domain, the entrainment is small and there is a direct balance between advective supply and biological export. The diffusive term is negligible in this integration, although the role of eddy transfers could be enhanced in an eddy-resolving model, as found in ^{14}C studies by Follows and Marshall (1996). Note that our advective transfer appears to be broadly in accord with the vertical and horizontal supply of nitrate shown in the GCM study by Sarmiento et al. (1993) (see their Fig. 6).

The advective supply of total nitrogen is separated into the geostrophic and Ekman terms in Fig. 11. The geostrophic advection supplies nutrients to the euphotic zone over the centre of the subtropical gyre, but elsewhere generally leads to a loss (Fig. 11a). This loss is due to the geostrophic transfer of surface, depleted $\mathcal{N}$ from low to high latitudes, and is similar to that found for inorganic carbon by Follows *et al.* (1996).

In contrast, the Ekman advection leads to a general supply of nutrients to the euphotic zone over much of the subpolar gyre, the northern flank of the subtropical gyre and the tropics, although there is a loss over the Gulf Stream (Fig. 11b). The supply reaches $2 \times 10^{-9}\,\mathrm{mol\,N\,m^{-2}\,s^{-1}}$ over the northern flank of the subtropical gyre, which is close to that found in the climatological diagnostics (replotted in Fig. 11c). The model shows a higher supply in the tropics, which may be due to the data study under-estimating the winter surface nitrate concentration there.

4.3.3. Sustaining export production towards the centre of the gyre

The supply of nutrients from the lateral transfer across the intergyre boundaries extends over a meridional scale reaching 1000 km into the interior of the subtropical gyre both in the climatological diagnostics and the model. How is this advective transfer of nitrate sustained away from the intergyre boundary, when the lifetime for nitrogen is very short in the summer euphotic zone?

Consider the nutrient cycle for a water column as it is swept southwards, following the geostrophic flow, into the interior of the subtropical gyre from the subtropical/subpolar boundary. The mixed layer is shallow in summer and deep in winter, and as the column moves into a warmer environment, the maximum thickness decreases each year – see the schematic shown in Fig. 12a. The nutrient is initially high in the winter mixed-layer due to the local intergyre supply of nutrients by the Ekman flow. The nutrients are rapidly removed during the summer (see the nitrogen cycle in Fig. 12b) as the lifetime of a nitrogen atom in the euphotic zone is only the order of a month. This surface removal leads to a spring and summer particulate fallout that is remineralised beneath the euphotic zone. As the mixed layer deepens again, the surface nutrients increase due to entrainment from the underlying seasonal thermocline including a fraction of nitrogen which was remineralised from the previous summers export. Hence, the initial nitrogen signal originating from the inter-gyre boundary persists over several years as the water column progresses into the gyre, despite being removed from the surface in summer (Fig. 12b). Note that if a longer surface lifetime, $1/\lambda$, is used, which may be more appropriate for the dissolved organic pool of nitrogen, then the nutrient signal will penetrate even further into the gyre.

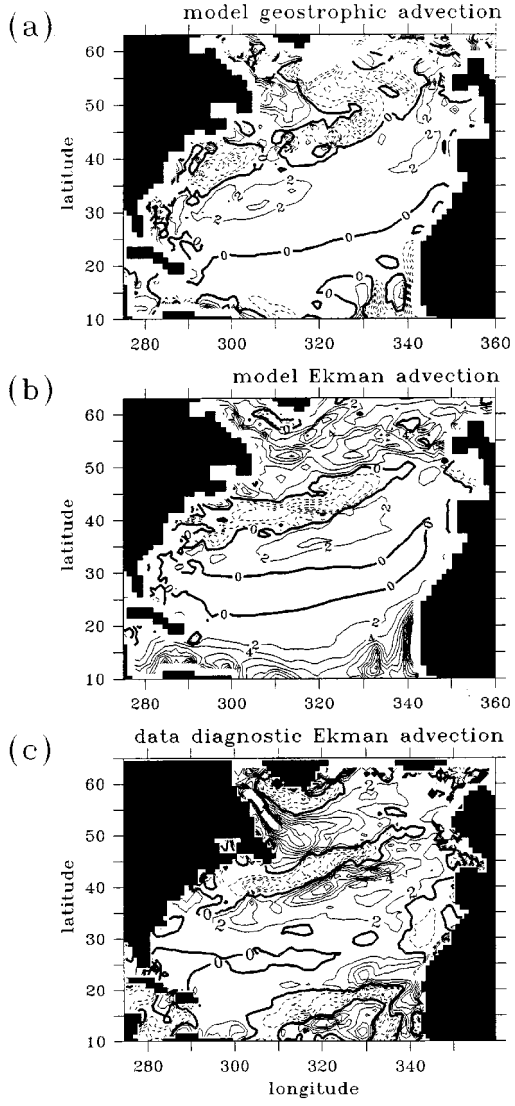

Fig. 11. Modelled advective supply of $\mathcal{N}$ (10^{-9} mol N m^{-2} s^{-1}) in the Ekman layer separated into (a) geostrophic advection and (b) Ekman advection. For comparison, the climatological data estimates of the Ekman transfer from Fig. 8a is replotted and shown in (c).

Archer et al. (1997) and Yamanaka and Tajika (1997), from models of dissolved organic carbon in the equatorial Pacific and global oceans, respectively, suggest a lifetime of semi-labile dissolved organic matter between 1 and 6 months in the surface ocean.

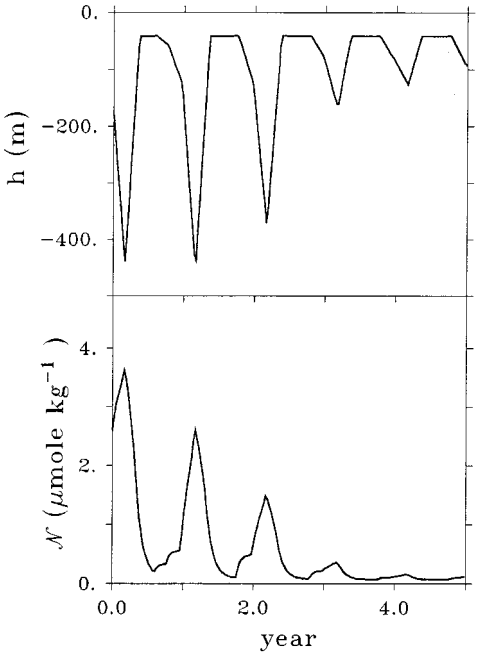

Fig. 12. A schematic figure showing (a) thickness of the mixed layer and (b) concentration of surface nutrients over several years following a water column. The water column is assumed to be swept from the northern flank of the subtropical gyre into the interior of the gyre (see Williams et al. (1995) for a Lagrangian example from the CME model). The mixed layer shallows each summer and deepens each winter, but with the maximum thickness decreasing each year. Using a one-dimensional version of the nitrogen cycle model, the surface nitrogen is found to be removed in summer, but reappears each winter due to the entrainment of nitrogen in the seasonal thermocline including remineralised fallout from the previous summer.

Therefore, we suggest that the productivity of the flanks of the subtropical gyre is determined by (i) the Ekman injection of nitrogen at the intergyre boundary, and (ii) the lifetime of nitrogen in the euphotic zone, which is partly controlled by the fraction of exported nitrogen re-entrained into the mixed layer during successive winters.

This hypothesis is now examined by artificially varying the remineralisation scale, z_*, within the GCM from the previous value of 400 m to a lower value of 100 m and an upper value of 2000 m. Fig. 13 shows, for these parameter values, both the advective contribution to export production and the particulate export across $z = -35$ m. As the remineralisation scale z_* decreases in magnitude, more nitrogen is retained within the seasonal boundary layer, which leads to an increase in the biological export and the advective transfer of nitrogen. Thus, the lateral extent of advective transfer of nitrogen into the subtropical gyre indeed appears to be controlled by how much nitrogen is retained within the seasonal boundary layer.

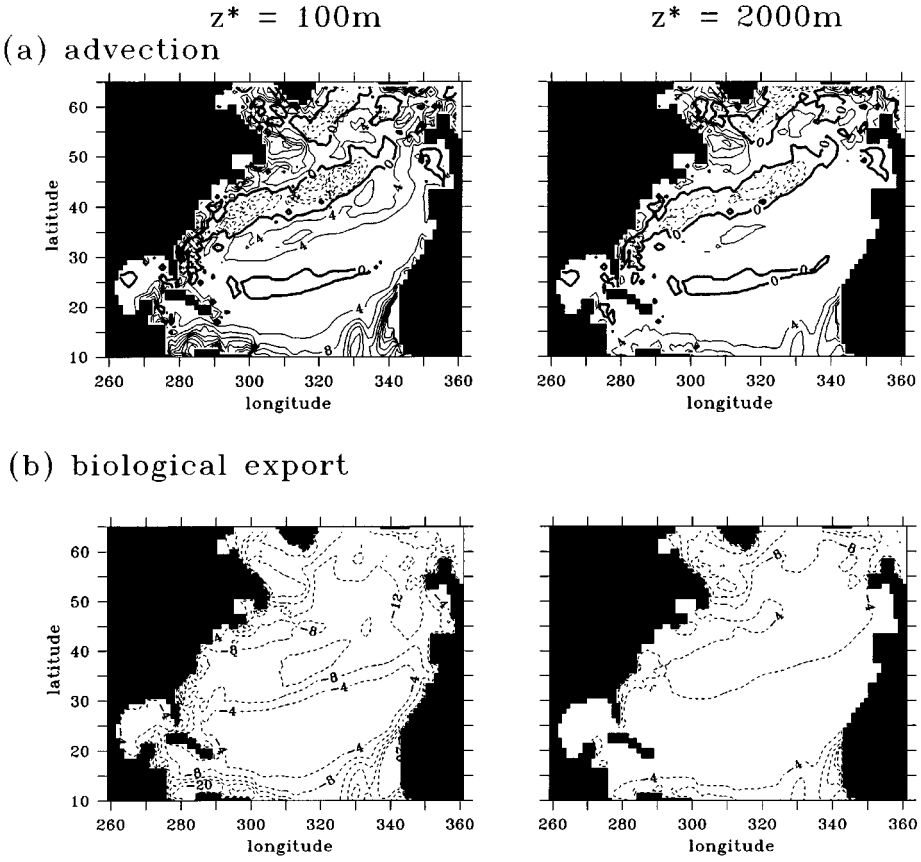

Fig. 13. Modelled fields of the biological export and advective supply of $\mathcal{N}$ (10^{-9} mol N m^{-2} s^{-1}) over the upper 35 m assuming a vertical remineralisation scale z_* of (a) 100 m and (b) 2000 m; compare with the previous case of $z_* = 400$ m shown in Fig. 10.

5. Discussion

Observations of ocean colour by remote sensing suggest that primary production is a maximum over upwelling regions, such as the subpolar gyre and tropics, reducing to lower values over the flanks of the subtropical gyre and with a minimum in the centre of the subtropical gyre. Assuming that some of the primary production is new production (and not entirely recycled production), this poses the question of how the implied new production is maintained and how new nutrients are supplied to the euphotic zone?

In this study, we focus on how the implied distribution of new production might be maintained through the gyre-scale circulation re-distributing nutrients. Our

climatological diagnostics suggest that Ekman upwelling supplies nutrients to the euphotic zone of the subpolar gyre, off the eastern boundary and over parts of the tropics. The accompanying *horizontal* Ekman volume fluxes likewise transfer nutrients from these upwelling regions to the flanks of the subtropical gyre. Our modelling study suggests that the lateral extent of enhanced surface nutrients and productivity, penetrating into the subtropical gyre from the intergyre boundary, is controlled by the mixed-layer cycle and the remineralisation of biological fallout within the seasonal thermocline.

Our climatological estimates suggest that the Ekman supply of nitrate ranges from 0.06 to 0.12 mol N m^{-2} yr^{-1} on the northern flank of the subtropical gyre.[4] This Ekman transfer of nitrate can support a new production from 0.4 to 0.8 mol C m^{-2} yr^{-1} over the northern flank of the subtropical gyre, assuming that the Redfield ratio is C : N = 105 : 15. In comparison, Sathyendranath *et al.* (1996) estimate that the annual primary productivity reaches 10 mol C m^{-2} yr^{-1} over the flanks of the subtropical gyre using remotely sensed chlorophyll (see Fig. 2). Assuming that this new production is a small fraction of the total production, with an f-ratio of 0.1–0.2 at these levels of primary production (Epply and Peterson, 1979), then this estimate implies a new production of 1–2 mol C m^{-2} yr^{-1}. Campbell and Aarup (1992) independently estimate a new production of 1 mol C m^{-2} yr^{-1} over the North Atlantic using remotely-sensed chlorophyll together with estimates of the downwards progression of the nutricline in summer from Strass and Woods (1991).

Our estimates of Ekman transfer are much smaller over the centre of the subtropical gyre and cannot directly account for much of the estimated new production near Bermuda of either 1 mol C m^{-2} yr^{-1} from sediment trap deployments by Altabet (1989) and Lohrenz et al. (1992), or 4 mol C m^{-2} yr^{-1} from tracer based estimates by Jenkins and Goldman (1985). However, our model integration suggests that geostrophic advection becomes significant in the centre of the gyre – within the model, the nutrients are transported into the subtropical gyre by the Ekman transfer at the intergyre boundaries and then transported to the centre of the gyre by the geostrophic flow. In addition, the advective supply from the intergyre boundaries may become more important for the dissolved organic pool of nitrogen, which has a longer lifetime in the euphotic zone.

The spatially-averaged annual Ekman supply of nitrate to the euphotic zone over the whole of the North Atlantic (from 5°N to 65°N) is positive and reaches 0.03 or 0.05 mol N m^{-2} yr^{-1} for the extrapolation and integral methods, respectively. This suggests an Ekman-induced biological pump of carbon into the ocean over the basin. Using a typical Redfield ratio to infer the associated soft-tissue pump, we determine an Ekman driven, biological uptake of carbon from the atmosphere of

[4] Note that Knap et al. (1986) estimate that atmospheric deposition over Bermuda only reaches an *upper* limit of 0.03 mol N m^{-2} yr^{-1} and the *in situ* fixation of dissolved nitrogen gas 3×10^{-5} mol N m yr^{-1}. Michaels *et al.* (1996) recently though have argued that nitrogen fixation might be an order of magnitude larger based on the observed nitrogen to phosphorus ratios in the Sargasso Sea.

0.07–0.09 Gt C yr^{-1} over the basin. This represents up to 17% of the total North Atlantic uptake of CO_2 estimated by Tans et al. (1990) from observations of atmospheric and surface ocean PCO_2(0.53 GT C yr^{-1} for the Atlantic basin north of 15°N). Note that our estimate is not for the total biological pump, as neither the non-Ekman supply of nitrogen nor the associated carbonate pump is included here.

In conclusion, our climatological diagnostics for the Ekman supply of nutrients imply values of new production over the subtropical gyre that are a significant fraction of the total inferred from independent methods. The lateral transfer of nutrients by geostrophic eddies may further enhance this dynamical supply into the subtropical gyre. While there are undoubtedly large errors in our climatological diagnostics, we believe that our signal of a strong intergyre transfer is robust, since the signal relies only on there being mid-latitude westerly winds and a poleward increase in surface nutrients during winter. Although our diagnostics have focussed on the North Atlantic, the Ekman and eddy transfers should also be important along intergyre boundaries in other basins and across zonal currents in the Southern Ocean.

Acknowledgements

RGW is grateful for support from MAS3-CT95-0043 (CLIVAMP) and MJF from NSF Grant OCE-9402308. We thank Mike Fasham for helpful feedback and Trevor Platt for kindly giving us access to the estimate of primary productivity displayed in Fig. 2.

Appendix A

A scale analysis is performed for the nutrient budget over the mixed layer to assess the importance of the various nutrient sources over summer and winter. Integrating Eq. (2) over the local instantaneous mixed-layer depth, h, (instead of the Ekman layer as in Eq. (6)) gives

$$h\frac{\partial \mathcal{N}_m}{\partial t} = -\int_{-h}^{0} \nabla\cdot(\mathbf{u}\mathcal{N})\,dz - \overline{w'\mathcal{N}'}_{z=0} + \overline{w'\mathcal{N}'}_{z=-h} + \int_{-h}^{0} \nabla\cdot(K\nabla\mathcal{N})\,dz + \int_{-h}^{0} S\,dz. \tag{A.1}$$

The magnitude of each of these terms is estimated for the supply into the subtropical gyre during winter and summer. The advective supply across the intergyre boundary is assumed to be dominated by the Ekman transfer:

$$-\int_{-h}^{0} \nabla\cdot(\mathbf{u}\mathcal{N})\,dz \sim -\mathbf{U}_e\cdot\nabla\mathcal{N}_m.$$

Air–sea deposition, $-\overline{w'\mathcal{N}'}_{z=0}$, is assumed to be typically $0.03\,\mathrm{mol\,N\,m^{-2}\,yr^{-1}}$ following the upper limit estimated by Knap et al. (1986).

The entrainment flux is given by

$$\overline{w'\mathcal{N}'}_{z=-h} = \Lambda(\mathcal{N}_{\mathrm{th}} - \mathcal{N}_{\mathrm{m}})\frac{\partial h}{\partial t}, \tag{A.2}$$

where $\mathcal{N}_{\mathrm{th}}$ are the nutrients entrained from the thermocline, and the Heaviside function, Λ, is defined as 1 when there is entrainment with $\partial h/\partial t > 0$ and otherwise 0. If there is an underlying linear nitrate profile, $\partial\mathcal{N}/\partial z$, that is initially continuous across the mixed-layer base, then the entrainment flux may be written as

$$\overline{w'\mathcal{N}'}_{z=-h} = -\Lambda\frac{\partial\mathcal{N}}{\partial z}h\left(1+\frac{h_{\mathrm{s}}^2}{h^2}\right)\frac{\partial h}{\partial t}.$$

This relation simplifies further as h_{s}/h, the ratio of summer and current mixed-layer depths, becomes small.

The diffusive supply of nutrients is separated into horizontal and vertical components with the horizontal and vertical diffusivity taken to be $K_{\mathrm{h}} = 1000\,\mathrm{m^{-2}\,s^{-1}}$, and $K_{\mathrm{v}} = 10^{-5}\,\mathrm{m\,s^{-1}}$.

The biological processes involving the consumption and export of nitrogen are simply represented by an exponential decay of the mixed-layer nitrate with a decay timescale of $(1/\lambda)$:

$$\int_{-h}^{0} S\,\mathrm{d}z = -h\lambda\mathcal{N}_{\mathrm{m}}.$$

The decay timescale is typically the order of a month in summer and increases to several months or years in winter for mid-latitudes.

Implementing the above parameterisations and estimates in Eq. (14), multiplying through by the density of seawater ρ, and assuming plausible scales for the subtropical gyre during winter and summer gives[5]

$$h\rho\frac{\partial\mathcal{N}_{\mathrm{m}}}{\partial t} = -\rho\mathbf{U}_{\mathrm{e}}\cdot\nabla\mathcal{N}_{\mathrm{m}} - \rho\overline{w'\mathcal{N}'}_{z=0} + \Lambda h\rho\frac{\partial\mathcal{N}}{\partial z}\frac{\partial h}{\partial t} + \rho h\,\nabla\cdot(K_{\mathrm{h}}\nabla\mathcal{N}_{\mathrm{m}})$$
$$-\rho K_{\mathrm{v}}\left(\frac{\partial\mathcal{N}}{\partial z}\right)_{z=-h} - h\rho\lambda\mathcal{N}_{\mathrm{m}}, \tag{A.3}$$

[5] We choose the following values for the parameters and gradients: the Ekman volume flux per unit length $V_{\mathrm{e}} \sim 1\,\mathrm{m^2\,s^{-1}}$ (equivalent to an Ekman velocity of $1\,\mathrm{cm\,s^{-1}}$ over a thickness of 100 m), $\partial\mathcal{N}_{\mathrm{m}}/\partial y \sim \partial y \sim 10^{-12}\,\mathrm{mol\,N\,kg^{-1}\,m^{-1}}$, $\partial\mathcal{N}_{\mathrm{m}}/\partial x \sim 0$, $\mathcal{N}_{\mathrm{m}} \sim 0.5\times10^{-6}\,\mathrm{mol\,N\,kg^{-1}}$, and, in the thermocline, $\partial\mathcal{N}/\partial z \sim 3\times10^{-8}\,\mathrm{mol\,N\,kg^{-1}\,m^{-1}}$ over the whole year. The mixed layer depth is assumed to be $h_{\mathrm{s}} \sim 50$ m in summer and $h \sim 200$ m in winter with the deepening occurring over 6 months. The biological decay time-scale is assumed to be $\lambda \sim 3\times10^{-7}\,\mathrm{s^{-1}}$ in the summer and only $10^{-8}\,\mathrm{s^{-1}}$ in winter.

where the terms on the right-hand side of (A.3) have the following values:

Winter:	2	1	20	0.2	0.3	−1,
Summer:	0.3	1	0	0.05	0.3	−10,

and all values are in units of 10^{-9} mol N m^{-2} s^{-1}. The terms on the right-hand side represent the nutrient supply integrated over the mixed layer due to Ekman advection, atmospheric deposition, entrainment, horizontal diffusion, vertical diffusion, and finally, biological consumption and export.

While these numbers are only crude estimates, they are useful in indicating the relative importance of the different terms in winter and summer. On a seasonal basis, the mixed-layer nitrate budget is dominated by entrainment during winter and biological export during summer. Advection in each season is an order of magnitude smaller than the leading processes. Thus the local, one-dimensional balance between entrainment and biological export captures the first order seasonal changes in surface nitrate.

However, integrating over the entire year, the biological export and entrainment terms largely oppose each other leaving advection with a more significant role in setting the annual nitrate distribution. This scale-analysis also suggests that horizontal advection and atmospheric deposition both dominate over vertical diffusion in the annual nitrate balance.

References

Altabet, M.A., 1989. Particulate new nitrogen fluxes in the Sargasso Sea. Journal of Geophysical Research 94, 12771–12779.

Archer, D., Peltzer, E.T., Kirchman, D. 1997. A time scale for cycling of DOC in equatorial Pacific surface waters. Global Biogeochemistry Cycles (submitted).

Bainbridge, A.E., 1981. GEOSECS Atlantic Expedition. vol. 1: Hydrographic Data 1972–1973. US Government Printing Office, Washington D.C.

Brewer, P.G., Takahashi, T., Williams, R.T., 1986. Transient Tracers in the Oceans (TTO) – Hydrographic Data and Carbon dioxide Systems with Revised Carbon Chemistry Data. Carbon Dioxide Information Center, U.S. Department of Energy, Oak Ridge, Tennessee.

Campbell, J.W., Aarup, T., 1992. New production in the North Atlantic derived from seasonal patterns of surface chlorophyll. Deep-Sea Research 39, 1669–1694.

Conkright, M.E., Levitus, S., Boyer, T.P., 1994. World Ocean Atlas 1994, Vol. 1: Nutrients, NOAA Atlas NESDIS 1, U.S. Dept. of Commerce, Washington D.C., 150 pp.

Dugdale, R.C., Goering, J.J., 1967. Uptake of new and regenerated forms of nitrogen in primary productivity. Limnology and Oceanography 12, 196–206.

Epply, Peterson, 1979. Particulate organic matter flux and planktonic new production in the deep ocean. Nature 282, 677–680.

Follows, M.J. Marshall, J.C., 1996. On models of bomb ^{14}C in the North Atlantic. Journal of Geophysical Research 101, 22577–22582.

Follows, M.J., Williams, R.G., Marshall, J.C., 1996. The solubility pump of carbon in the subtropical gyre of the North Atlantic. Journal of Marine Research 54, 605–630.

Fukumori, I., Martel, F., Wunsch, C., 1991. The hydrography of the North Atlantic in the early 1980s. An atlas. Progress in Oceanography 27, 1–110.

Glover, D.M., Brewer, P.G., 1988. Estimates of wintertime mixed layer nutrient concentrations in the North Atlantic. Deep-Sea Research 35, 1525–1546.

Holland, W.R., Bryan, F.O., 1994. Sensitivity studies on the role of the ocean in climate change. In: Malanotte-Rizzoli, P., Robinson, A.R. (Eds.), Ocean Processes in Climate Dynamics: Global and Mediterranean Examples. Kluwer Academic Publishers, Dordrecht, Netherlands, pp. 111–134.

Isemer, H.J., Hasse, L., 1987. The Bunker Climate Atlas of the North Atlantic Ocean, Vol. 2. Springer, Berlin.

Jenkins, W.J., Goldman, J.C., 1985. Seasonal oxygen cycling and primary production in the Sargasso Sea. Journal of Marine Research 43, 465–491.

Knap, A., T. Jickells, A. Pszenny, Galloway, J., 1986. Significance of atmospheric-derived fixed nitrogen on productivity of the Sargasso Sea. Nature 320, 158–160.

Leach, H., 1990. Interannual variability in the upper ocean in the North Atlantic, summer 1983 and 1986. Deep-Sea Research 37, 1169–1175.

Ledwell, J.R., Watson, A. J., Law, C.S., 1993. Evidence for slow mixing across the pycnocline from an open-ocean tracer-release experiment. Nature 364, 701–703.

Levitus, S., 1982. Climatological Atlas of the World Ocean. NOAA prof. Paper No. 13, Washington D.C., 173 pp.

Lohrenz, S.E., Knauer, G.A., Asper, V.L., Tuel, M., Michaels, A.F., Knap, A.H., 1992. Seasonal variability in primary production and particle flux in the northwestern Sargasso Sea: U.S. JGOFS Bermuda Atlantic Time-series Study. Deep-Sea Research 39, 1373–1391.

Martin, J.H., Knauer, G.A., Karl, D.M., Broenkow, W.W., 1987. VERTEX: Carbon cycling in the northeast Pacific. Deep-Sea Research 34, 267–285.

McClain, C.R., Firestone, J., 1993. An investigation of Ekman upwelling in the North Atlantic. Journal of Geophysical Research 98, 12327–12339.

McGillicuddy, D.J., Robinson, A.R., 1998. Eddy-induced nutrient supply and new production in the Sargasso Sea. Deep-Sea Research (in press).

Michaels, A.F., Sarmiento, J.L., Prospero, J.M., 1996. Excess nitrate and the rate of nitrogen fixation in the Sargasso Sea. Abstract, 1966 AGU Ocean Sciences Meeting, Eos (suppl.), 76.

Munk, W.H., 1966. Abyssal recipes. Deep-Sea Research 13, 707–730

Najjar, R.G., Sarmiento, J.L., 1992. Downward transport and fate of organic matter in the ocean: Simulations with a general circulation model. Global Biogeochemistry Cycles 6, 45–76.

Neumann, G., 1940. Die ozeanographischen Verhaeltnisse an der Meeresoberflaeche im Golfstromsektor noerdlich und nordwestlich der Azoren. Ann. Hydr. Marit. Meterol. 68, Juni, Beiheft, 87pp.

Paltridge, G.W., Platt, C.M.R., 1976. Radiative Processes in Meteorology and Climatology. Elsevier, Amsterdam.

Sarmiento, J. L., Slater, R.D., Fasham, M.J.R., Ducklow, H.W., Toggweiler, J.R., Evans, G. T., 1993. A seasonal three-dimensional ecosystem model of nitrogen cycling in the North Atlantic euphotic zone. Global Biogeochemical Cycles 7(2), 417–450.

Sathyendranath, S., Longhurst, R.S.A., Caverhill, C.M., Platt, T., 1995. Regionally and seasonally differentiated primary production in the North Atlantic. Deep-Sea Research I 42, 1773–1802.

Strass, V.H., Woods, J.D., 1991. New production in the summer revealed by the meridional slope of the deep chlorophyll maximum. Deep-Sea Research 38, 35–56.

Tans, P.T., Fung, I.Y., Takahashi, T., 1990. Observational constraints on the global atmospheric budget. Science 247, 1431–1438.

Taylor, A.H., Stevens, J.A., 1980. Seasonal and year-to-year variations in surface salinity at the nine North Atlantic Ocean Weather Stations. Oceanologica Acta 3, 421–430.

Williams, R.G., Spall, M.A., Marshall, J.C., 1995. Does Stommel's mixed layer 'Demon' work? Journal of Physical Oceanography 25, 3089–3102.

Yamanaka, Y., Tajika, E. 1997. The role of dissolved organic matter in the marine biogeochemical cycle: studies using an ocean biogeochemical general circulation model. Global Biogeochemistry Cycles (submitted).